Defence Science Journal, Vol. 73, No. 2, March 2023, pp. 231-240, DOI : 10.14429/dsj.73.18721

Effect of Vanadium Addition on Structure and Soft Magnetic Properties of Nanocrystalline FeCoZrBCu Melt Spun Alloys

D. Atchyut Kumar[#], Saijyothi N.[$], D. Arvindha Babu[$,*], J. Arout Chelvane[$], M. Manivel Raja[$] and T.K. Nandy[$]

[#]*Indian Institute of Technology, Hyderabad – 502284, India*
[$]*DRDO-Defence Metallurgical Research Laboratory, Hyderabad – 500 058, India*
[*]*E-mail: darvindhababu@gmail.com*

ABSTRACT

In this study, glass forming ability, structure and soft magnetic properties of melt spun ribbons of $(Fe_{1-x}Co_x)_{88-y}V_yZr_7B_4Cu_1$ alloys with compositions $x_{0.1}y_2$, $x_{0.1}y_4$ and $x_{0.1}y_6$ & $x_{0.35}y_2$, $x_{0.35}y_4$ and $x_{0.35}y_6$ have been investigated. All alloys were found to be fully amorphous after melt spinning. Annealing of amorphous ribbons of $x_{0.1}$ series alloys leads to the formation of bcc α-Fe(Co) phase and Fe_2Zr phase in the amorphous matrix, while annealing of amorphous ribbons of $x_{0.35}$ series alloys, leads to the formation of only bcc α-Fe(Co) phase in the amorphous matrix. High precision lattice parameter calculations revealed that V addition influences the phase formation in low Co containing $x_{0.1}$ alloys. It leads to low volume fraction of bcc α-Fe(Co) phase and promotes Fe_2Zr phase. A higher Co content increases the Curie temperature (T_c) of amorphous phase, while V addition decreases the T_C of amorphous phase in both $x_{0.1}$ and $x_{0.35}$ series of alloys. Saturation magnetization (M_s) of $x_{0.35}$ alloys are higher than of $x_{0.1}$ alloy due to higher Co content and the M_s decreases with increasing V content due to its non-magnetic nature. Coercivity was found to be increased with annealing in $x_{0.35}$ alloys due to the low volume fraction formation of bcc α-Fe(Co) phase and Fe_2Zr phase. The coercivity decreases with increasing V addition in $x_{0.35}$ alloys as spun ribbons and a lowest coercivity of 0.13 Oe has been obtained in $x_{0.35}y_6$ alloy which is one of the lowest among FeCoZrBCu alloys reported.

Keywords: Amorphous and nanocrystalline soft magnetic material; Gass forming ability and metallic glass

1. INTRODUCTION

FINEMET (Fe-Si-B-Nb-Cu), NANOPERM (Fe-Zr-B-Cu) and HITPERM (Fe(Co)-Zr-B-Cu) are nanocrystalline soft magnetic materials prepared by partial devitrification of amorphous precursors and these materials have attracted much attention of the researchers worldwide due to their excellent soft magnetic properties and their wide variety of applications. They are used in pulsed transformers on defence and space systems in devices such as magnetic amplifiers, DC-DC converter, SMPS, common mode choke, wind generator and solar converter.

Fe-Si-B-Nb-Cu alloys, developed by Yoshizawa[1], *et al.* and Fe-Zr-B-Cu alloys, developed by Suzuki[2], *et al.* are not suitable for the applications above 250 °C[3] due to their low Curie temperature although they possess a good combination of soft magnetic properties such as higher permeability (μ_r) and saturation magnetization (M_s) combined with low coercivity (H_c) and core loss. Whereas Fe(Co)-Zr-B-Cu alloys developed by Willard[4], et al. has low permeability, but its Curie temperature (T_c) and saturation magnetization (M_s) are appreciably high as compared to other nanocrystalline soft magnetic materials[3, 5-7]. Hence there is a continued research being pursued to improve the soft magnetic properties of these alloys.

Received : 21 November 2022, Revised : 10 December 2022
Accepted : 02 February 2023, Online published : 06 April 2023

Numerous studies on investigation of structure and soft magnetic properties of Fe(Co)-Zr-B-Cu alloys have been carried out by various researchers by varying the composition, alloying additions and heat treatment. Babu[8], et al. have reported the influence of melt-spinning parameters on the structure and soft magnetic properties of $(Fe_{0.65}Co_{0.35})_{88}Zr_7B_4Cu_1$ alloy. Melt spun ribbons processed at various wheel speeds have profound influence on soft magnetic properties through formation of various microstructures. Subsequent annealing was not effective on improving the soft magnetic properties. They also have reported the structure and soft magnetic properties of melt spun $(Fe_{1-x}Co_x)_{88}Zr_7B_4Cu_1$ alloys with x = 0.2, 0.35, 0.5, and 0.6 compositions[9]. They established that the composition of FeCo phase is almost same as ($Fe_{73}Co_{27}$) irrespective of initial compositions. They also reported that M_s value peaked at 0.35 at% Co and the coercivity increased with increase in Co content. An effort was taken by Parsons and Suzuki[10] to reduce the alloying elements to increase the M_s value above 2T while achieving H_c as low as 9.3 A/m. Li[11], *et al.* have studied $(FeCo)_x$BSiVCuY amorphous/nanocrystalline alloy system and found a large annealing temperature window to obtain dual-phase with improved magnetic properties.

The alloying additions were reported by various investigators. Fan[12], et al. have reported the effect of Ni addition on microstructure and soft magnetic properties of nanocrystalline alloys of $(Fe_{0.7}Co_{0.3-x}Ni_x)_{88}Zr_7B_4Cu_1$, where

x=0, 0.1, 0.2, and 0.3. The results show that the substitution of Ni for Co increases the thermal stability and reduces the magneto-crystalline anisotropy. They also reported that these alloys exhibit B_s of 1.54-1.79 T, H_c of 17-20 A/m and low core loss of 9.1-11.1 W/kg at 1 T and 400 Hz, respectively. Yu[13], *et al.* have reported the effect of Mo addition on the thermal stability, microstructure and magnetic properties of $Fe_{80-x}Co_xZr_{10-y}Mo_yB_9Cu_1$ (x=10, 20, 30; y=0, 2) alloys. Mo addition decreases the activation energies of primary crystallization. Mo addition was found to influence the presence of Co in either amorphous or α-Fe phase. Mitra[14], *et al.* have reported Al and Si addition in FeCoZrBCu alloys and reported that annealing of $Fe_{40}Co_{40}Cu_{0.5}Zr_9Al_2Si_4B_{4.5}$ alloy at 873 K for 15 min. develops nanocrystalline structure with high curie temperature, high saturation magnetization and good AC soft magnetic properties.

Blazquez[15], *et al.* have reported the magnetic permeability of $(FeCoGe)_{88}Zr_6B_5Cu_1$ alloys and found that as nanocrystallization progresses, room temperature magnetic permeability (μ) decreases, but increases at high temperatures, thus leading to an improvement of its thermal stability. Srivastava[16], *et al.* have reported, understanding the effect of Hf on thermal stability and glass forming ability of $Fe_{57.2}Co_{30.8}Zr_{7-x}Hf_xB_4Cu_1$ (x=3, 5, and 7) metallic glasses. This study indicated relative deterioration in thermal stability and GFA with an increase in Hf content at the cost of Zr.

It is worth mentioning here that in Permandur FeCo alloys, Vanadium (V) is added to increase the ductility thereby workability. However, the magnetic softness can be achieved in FeCoV alloys by adopting suitable heat treatment schedule[17]. Since FeCoZrBCu alloys were developed based on FeCo Permandur alloys and effect of V addition in FeCoZrBCu alloys has not been reported in the literature, there is a scope for studying the effect of V addition in nanocrystalline FeCoZrBCu alloys. Therefore, the present investigation deals with the study of V addition on the structure and soft magnetic properties of Fe(Co)-Zr-B-Cu based amorphous and nanocrystalline alloys. The alloy systems under consideration in the present study, are $(Fe_{1-x}Co_x)_{88-y}V_yZr_7B_4Cu_1$ with x = 0.1 and 0.35 series and y = 2, 4 and 6 and these alloys are designated as $x_{0.1}y_2$, $x_{0.1}y_4$ and $x_{0.1}y_6$ & $x_{0.35}y_2$, $x_{0.35}y_4$ and $x_{0.35}y_6$ respectively.

2. EXPERIMENTAL DETAILS

Two series of alloys with nominal composition of $(Fe_{1-x}Co_x)_{88-y}V_yZr_7B_4Cu_1$ with $x_{0.1}y_2$, $x_{0.1}y_4$ and $x_{0.1}y_6$ *($x_{0.1}$ series)* & $x_{0.35}y_2$, $x_{0.35}y_4$ and $x_{0.35}y_6$ *($x_{0.35}$ series)* alloys were prepared using vacuum arc melting furnace (at a vacuum of 10^{-4} mbar). Rapidly solidified ribbons of 20 – 50 μm thick and 2-5 mm wide have been prepared using a vacuum melt spinning unit. Initially, a high vacuum of 4×10^{-4} mbar was achieved in the melt spinning chamber followed by backfilling of pure argon gas up to a pressure slightly below 1 atmospheric pressure. Subsequently, the melt spinning experiments were carried out with the processing parameters given in Table 1. As spun ribbons were annealed in a tubular furnace under a vacuum of 1×10^{-5} mbar at different temperatures (500 – 660 °C) for an hour. The experimental parameters were selected based on our previous work[9].

Structural characterization of as spun and annealed ribbons was carried out using by using X-Ray diffractometer (PHILIPS PW1830 XRD) using Cu-K_α (λ = 1.54056 Å) radiation. Microstructural characterization was done using transmission electron microscope (TEM) (Model: FEI Tecnai-20 G2, Amsterdam, Netherlands). A differential scanning calorimeter (DSC, Model: TA DSC Q400) (at a heating rate of 20 °C/ min) was used to evaluate the thermal stability of the as spun ribbons. Saturation magnetization (at an applied field of 5 kOe) and thermomagnetic curves (at an applied field of 50 Oe) were obtained from Vibrating Sample Magnetometers (VSM) of ADE EV7 and LAKESHORE CRYOTRONICS 7404, respectively. A coercimeter (FÖSTER-KOERZIMET 1.095) was used to evaluate the coercivity of as spun and annealed ribbons.

3. RESULTS AND DISCUSSION

3.1 Glass Forming Ability, Structure and Thermal Stability

The XRD patterns of as spun ribbons of $x_{0.1}$ series and $x_{0.35}$ series alloys prepared at a wheel speed of 47 m/s are shown in Fig. 1 (a) & (b). From the XRD patterns, one can observe the existence of only broad halo peak without any sharp peak in all alloys which confirms the presence of only amorphous phase. Earlier, amorphous phase formation was reported in similar alloy without V addition, melt spun at similar experimental conditions[9]. This proves that V addition in these alloys does not seem to affect the glass formation.

Figure 2a shows the DSC thermograms of as spun ribbons of $x_{0.1}y_2$, $x_{0.1}y_4$ and $x_{0.1}y_6$ alloys obtained at a heating rate of 20 °C/min. It can be observed from the DSC thermograms that all alloys exhibit only one exothermic peak which corresponds to the crystallization of amorphous phase. The onset temperature of crystallization for $x_{0.1}y_2$ alloy is 559 °C which increases with increase in V content. Figure 2(b) shows DSC thermograms of as spun ribbons of $x_{0.35}y_2$, $x_{0.35}y_4$ and $x_{0.35}y_6$ alloys. In these alloys also, only one exothermic peak is observed as similar to $x_{0.1}$ alloys and it also shows the increase in onset of crystallization temperatures with increase in V content. These onset of crystallization temperatures, are higher than that of $x_{0.35}$ alloy without Vanadium which was reported as 506 °C in our earlier study[9]. One can also notice that the onset temperatures of $x_{0.1}$ alloys are higher than that of $x_{0.35}$ alloys. The effect of V addition is well pronounced on crystallization behaviour at lower content and then the difference in onset temperature was found to be decreased at higher V content. It infers that a small addition of V is advantageous as it improves the stability of amorphous phase without affecting the magnetic properties.

Table 1. Experimental parameters used in melt spinning experiments

Alloy	Wheel speed (m/s)	Ejection pressure (psi)	Crucible orifice diameter (mm)	Ribbon thickness (μm)
$x_{0.1}$ and $x_{0.35}$	47	2	0.8	20-50

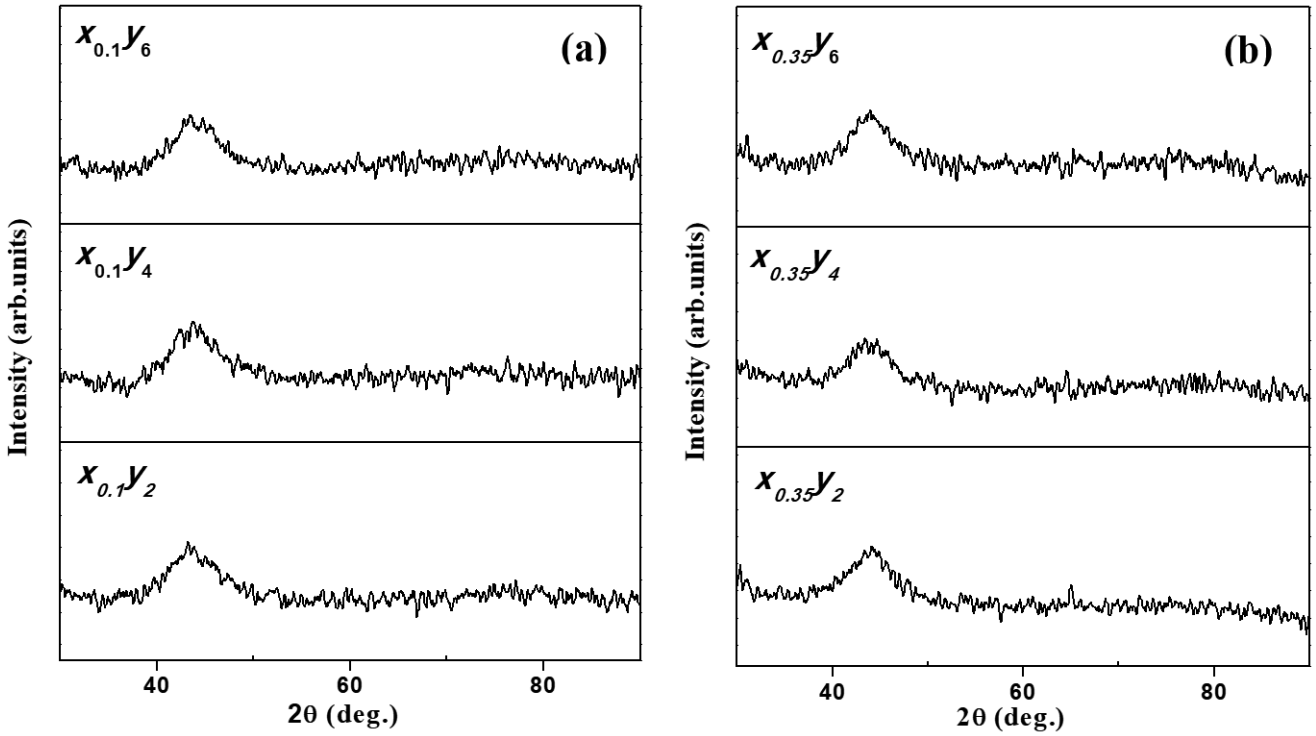

Figure 1. XRD patterns of (a) $x_{0.1}$ and (b) $x_{0.35}$ series alloys as spun ribbons with different vanadium content.

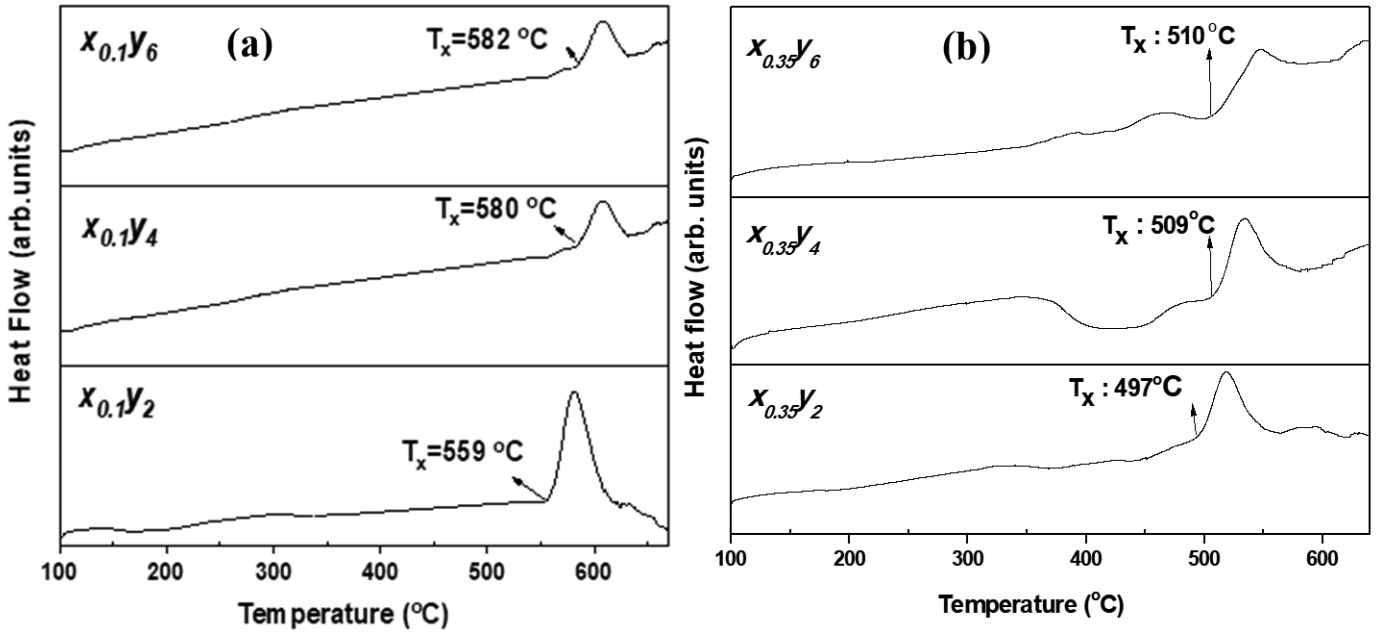

Figure 2. DSC thermographs of as spun ribbons of (a) $x_{0.1}$ and (b) $x_{0.35}$ series alloys obtained at a heating rate of 20 °C/min.

The increase in crystallization temperature may be correlated with melting temperature of the elements added. In case of Co having lower melting point (1495°C) replaced for high melting point Fe (1536°C), the onset of crystallization temperature decreases. In case of V having high melting point (1900°C) than that of Fe, the increase in the onset temperature is only marginal due to the low weight fraction of V added.

V addition in FINEMET alloys ($Fe_{73.5}Cu_1B_{13}Si_{9.5}Nb_{3-x}$ where x = 0, 1 and 1.5) have been reported to increase the glass forming ability (GFA) considerably. Since these alloys exhibit glass transition temperature (T_g), the GFA was calculated through undercooled regime (ΔT) which is calculated as the difference between the crystallization temperature (T_x) and T_g. The ΔT (i.e, GFA) increased to 132 °C for x = 1.5 alloy from 99 °C for x = 0 alloy. In the present study, as T_g was not observed, theoretical methods for calculating the GFA needs to be resorted. Hence, to understand the effect of V addition in these alloys, GFA of the alloys have been calculated using a theoretical parameter named P_{HSS} parameter proposed by Rao[18], *et al.* which is the product of three thermodynamic quantities viz. enthalpy of chemical mixing (ΔH^{chem}), mismatch entropy (ΔS_σ) and configurational entropy (ΔS_c). Many reports have

been published validating this method for Fe based alloys[18,22]. P_{HSS} can empirically be given as,

$$P_{HSS} = \Delta H^{chem}\left(\Delta S_{\sigma} / k_B\right)\left(\Delta S_c / R\right) \quad (1)$$

Table 2. Theoretical and experimental GFA parameters and thermo-magnetic properties of the alloys

Alloy composition	P_{HSS} (kJ/mol)	Onset crystallisation temperatures (T_x) (°C)	Curie temperature (T_C) (°C)
$x_{0.1}y_0$	-0.98	-	-
$x_{0.1}y_2$	-1.01	559	198
$x_{0.1}y_4$	-1.04	580	167
$x_{0.1}y_6$	-1.07	582	121
$x_{0.35}y_0$	-0.83	506	-
$x_{0.35}y_2$	-0.85	497	520
$x_{0.35}y_4$	-0.88	509	460
$x_{0.35}y_6$	-0.90	510	420

where ΔH^{chem} is the enthalpy of chemical mixing, ΔS_{σ} is the mismatch entropy, ΔS_c is the configurational entropy, k_B is Boltzman constant and R is gas constant. The value of enthalpy of chemical mixing (ΔH^{chem}) calculated from Miedema's semi-empirical model[19,20]. The mismatch entropy was calculated from the empirical relation given by Mansoori[21], et al. The configurational entropy was calculated using a formula,

$$\Delta S_c = -R\sum_{i=1}^{n} x_i \ln x_i \quad (2)$$

where R is the gas constant and x is the mole fraction. Alloys with high GFA will have high P_{HSS} values on the negative side. P_{HSS} values for $x_{0.1}$ and $x_{0.35}$ alloys have been calculated and given in the Table 2. One can see that the P_{HSS} value increases with increase in V content in both $x_{0.1}$ and $x_{0.35}$ alloys and however the P_{HSS} values of $x_{0.1}$ alloys are marginally higher that of $x_{0.35}$ alloys. It is also to be noted that though V addition increases the P_{HSS} values and Co content decreases it. In the alloys studied, P_{HSS} values decreases with increasing Co and it increases marginally with increasing V. This indicates that the Co addition decreases the GFA and V addition increases it in the respective alloys. Also the increase in onset of crystallization temperature (T_x) observed in DSC results indicates the increase

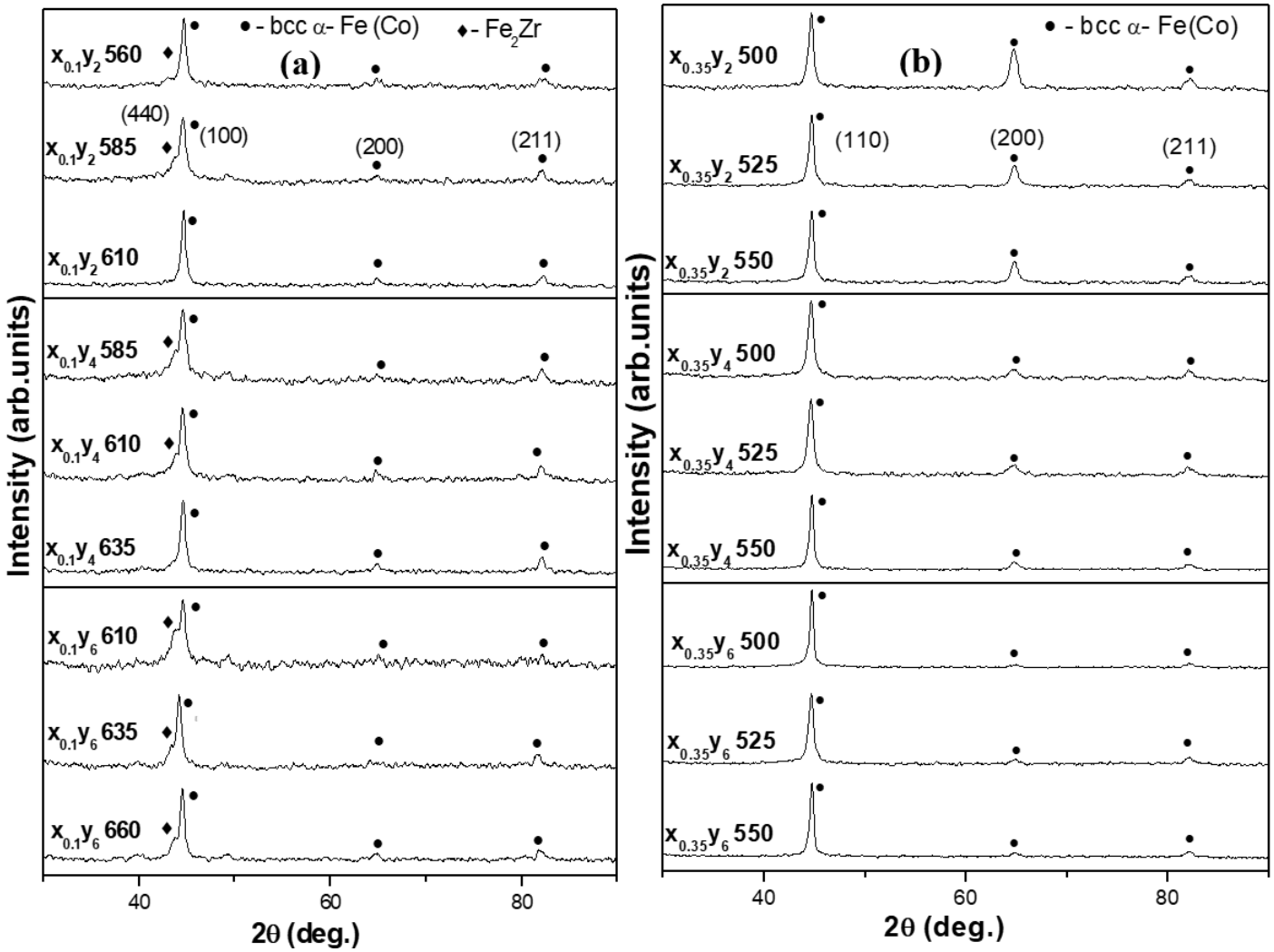

Figure 3. XRD patterns of annealed ribbons of (a) $x_{0.1}$ and (b) $x_{0.35}$ series alloys at different temperatures for an hour.

of thermal stability of amorphous phase and it is also used in ΔT (=T_x-T_g, where T_g is glass transition temperature) to calculate the GFA where high T_x suggests high GFA. The T_x behavior with respect to Co and V addition is in agreement with P_{HSS} results.

Figure 3(a) shows the XRD patterns of annealed ribbons of $x_{0.1}y_2$, $x_{0.1}y_4$ and $x_{0.1}y_6$ alloys. It can be noted that the patterns exhibit sharp reflections which proves the formation of crystalline phases from amorphous phase. Indexing of theses peaks reveal that the formation of bcc α-Fe(Co) phase and Fe_2Zr phases. A shallow broad base at the base of the (110) peak of bcc α-Fe(Co) phase proves that the amorphous phase transformation into crystalline phases is not completed. The general behaviour in Fe(Co)ZrBCu materials reported in the literature is that initially bcc α-Fe(Co) phase forms from amorphous phase upon annealing which gets converted into Fe_3Zr phase at high temperatures. However, recently it is reported in $Fe_{86}Zr_7B_6Cu_1$ alloys that increasing Zr from 7 to 9 at%[22], an intermediate phase of Fe_2Zr phase forms before Fe_3Zr phase forms. The similar behaviour is also observed in the present study. To get the volume fraction of the amorphous phase and bcc α-Fe(Co) phase qualitatively in the annealed ribbons, area fraction of the each phase is calculated after deconvoluting both phases using Gaussian peak fitting. It is to be noted that the volume fraction of the bcc α-Fe(Co) phase is in the range of 60 to 70 % and the amorphous phase is in the range of 20 to 35 %.

Figure 3b shows the XRD patterns of annealed ribbons of $x_{0.35}y_2$, $x_{0.35}y_4$ and $x_{0.35}y_6$ alloys at different temperatures for an hour. Unlike, $x_{0.1}$ alloys, all annealed ribbons of $x_{0.35}$ alloy have only one crystalline phase i.e. bcc α-Fe(Co) phase along with the amorphous phase. No trace of Fe_2Zr phase and amorphous phase are observed in all annealed ribbons. This suggests that annealing leads to the formation of only bcc α-Fe(Co) phase from amorphous phase.

Figure 4 shows the precision lattice parameter values as a function of annealed temperature of all ribbons. The Precision lattice parameter values (a_0) (determined using Nelson-Riley Extrapolation method[23]) of bcc α-Fe(Co) phase of all annealed ribbons are in the range of 0.286 nm to 0.289 nm. One can

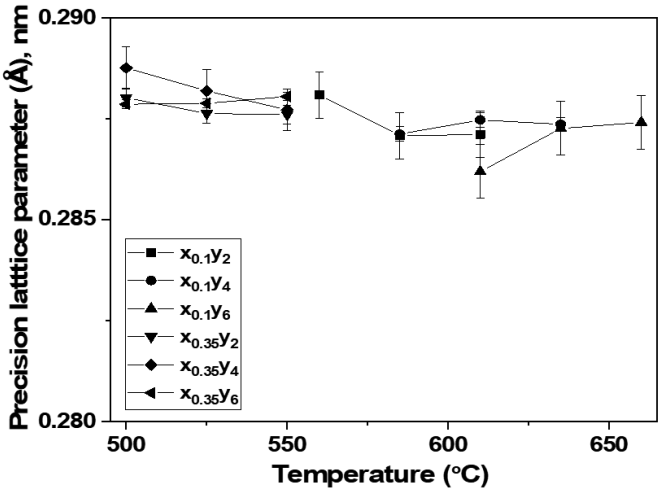

Figure 4. Precision lattice parameter as a function of annealed temperature of all ribbons.

see that a_0 values of $x_{0.1}$ alloys are low and are in the range of 0.286 to 0.287 nm. As the $x_{0.1}$ alloys are having Fe as a major constituent element with low Co content, bcc α-Fe(Co) phase's a_0 values are approximately equal to the a_0 value of pure iron (Fe) which is 0.2866 nm. However, for $x_{0.35}$ alloys a_0 values are higher than that of $x_{0.1}$ alloys and are in the range of 0.287 to 0.289 nm. Babu[9] et.al. reported that the a_0 value of $x_{0.35}y_0$ as 0.2869 nm which proves that the V addition increases the lattice parameter. $x_{0.1}$ and $x_{0.35}$ alloys having the same composition except the Co content variation and hence V addition in the presence of Co seem to increase the a_o value.

This can be explained by the enthalpy of mixing (ΔH_{mix}) calculated from the Miedema's model which gives that ΔH_{mix} for Fe-V is -29.8 kJ/mol, Co-V is -59.8 kJ/mol, V-Zr is + 15kJ/mol and for V-B is -248 kJ/mol. It is to be noted that ΔH_{mix} of V in Cu is not considered as the concentration of Cu in this alloy is very less. Although V in B has very highly negative value of $\Delta H_{mix,}$ the concentration of B in this alloy is very less i.e. 1 wt% and hence the interaction B atoms with other elements may be scarce. The positive value of ΔH_{mix} for V in Zr repels the V atoms in the amorphous matrix and ΔH_{mix} of Co-Zr (-208 kJ/mol) is higher than that of ΔH_{mix} of Fe-Zr (-124 kJ/mol), Zr gets attracted to the bcc α-Fe(Co) phase because of the presence of higher Co content in $x_{0.35}$ alloys during phase transformation of amorphous to bcc α-Fe(Co) phase in annealing. The chances of V atoms to go into the α-Fe(Co) phase are very low as ΔH_{mix} for Fe-V (-29.8 kJ/mol) and Co-V (-59.8 kJ/mol) have lower negative values than that of ΔH_{mix} of Co-Zr and Fe-Zr. Therefore, Zr having higher atomic size (2.05Å) than that of Fe (1.26Å) and Co (1.18Å), presence of Zr in bcc α-Fe(Co) phase increases lattice parameter in $x_{0.35}$ alloys as compared to $x_{0.1}$ alloys.

It is interesting to note that V addition in $x_{0.1}$ alloys leads to the formation of nanocrystalline bcc α-Fe(Co) phase as a major phase and Fe_2Zr phase as a minor phase. However, in $x_{0.35}$ alloys, only bcc α-Fe(Co) phase is formed and Fe_2Zr phase does not form. In case of FeCoZrBCu alloys, annealing only forms only bcc α-Fe(Co) phase and many researchers have reported in similar lines[6-7].

The unusual behaviour of the formation of Fe_2Zr phase formation in $x_{0.1}$ alloys can be explained using the precision parameter (a_0) calculations. As a_0 values of bcc α-Fe(Co) phase formed on annealing of $x_{0.1}$ alloys, are equivalent to the pure Fe values, V (1.44Å) and Zr (2.05 Å) being the bigger size atoms are expected to remain in the amorphous phase. As ΔH_{mix} of V in Zr is positive (+ 15kJ/mol) and ΔH_{mix} of Zr in Fe is highly negative (-124 kJ/mol), Zr is repelled by V and attracted by Fe. ΔH_{mix} of Zr in Co is still highly negative (-208 kJ/mol) and as Co atomic fraction is less as compared to Fe, Co-Zr interaction is highly unlikely. Therefore, Fe-Zr interaction is highly likely which may possibly be the reason for the formation of Fe_2Zr in $x_{0.1}$ alloys. As it was proved earlier, in case of $x_{0.35}$ alloys, the Zr atoms go into the nanocrystalline bcc α-Fe(Co) phase on annealing due to the presence of Co atom in α-Fe(Co) phase, Fe-Zr interaction in the amorphous matrix is unlikely and hence Fe_2Zr phase does not form.

The crystallite size of bcc α-Fe(Co) phase was calculated using Debye-Scherrer formula and the calculated crystallite

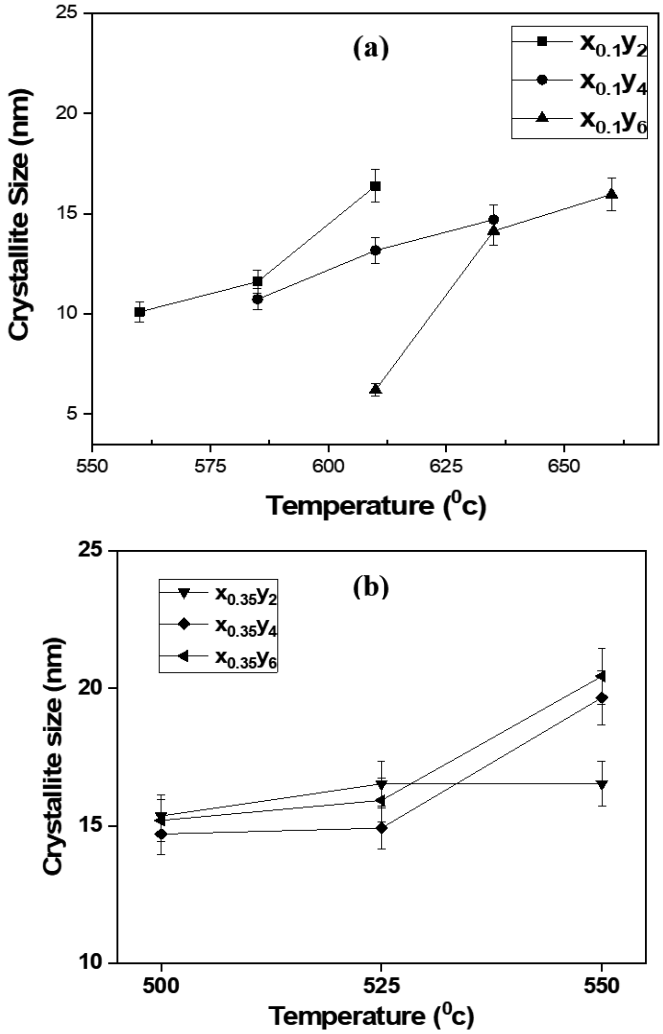

Figure 5. Crystallite size of: (a) $x_{0.1}$ and (b) $x_{0.35}$ alloys as a function of annealing temperature.

sizes of annealed ribbons are plotted as a function of annealing temperature which are given in the Fig. 5 (a&b) for $x_{0.1}$ and $x_{0.35}$ series alloys, respectively. In case of $x_{0.1}$ alloys, the crystallite size increases with increasing annealing temperature and the minimum and maximum crystallite sizes obtained are 6 nm and 16.4 nm, respectively. In case of $x_{0.35}$ alloys, the increase in crystallite sizes with annealing temperatures is not as high as compared to $x_{0.1}$ alloys. However, the observed crystallite sizes of $x_{0.35}$ alloys are in the range of 14.7 nm to 20.5 nm which is much higher than that of $x_{0.1}$alloys. Babu[9], et.al. have reported the maximum grain size of 22.11 nm in $x_{0.35}y_0$ alloy which suggests that V addition does not influence much in the grain growth of bcc α-Fe(Co) phase of $x_{0.35}$ alloys.

Figure 6(a) shows the TEM bright field (BF) image of as spun ribbon of $x_{0.1}y_2$ alloy and the inset shows the corresponding selected area electron diffraction pattern (SAD). From the TEM BF image, one can see a featureless contrast and the bright halo in the SAD patterns which prove that the as spun ribbon is completely amorphous corroborating the XRD results. Figure 6b shows the TEM BF image of $x_{0.1}y_2$ alloy ribbon annealed at 610 °C and the inset shows the corresponding SAD pattern. One can see that the uniform distribution of nanograins in the amorphous matrix with the size ranging from 10 – 20 nm and

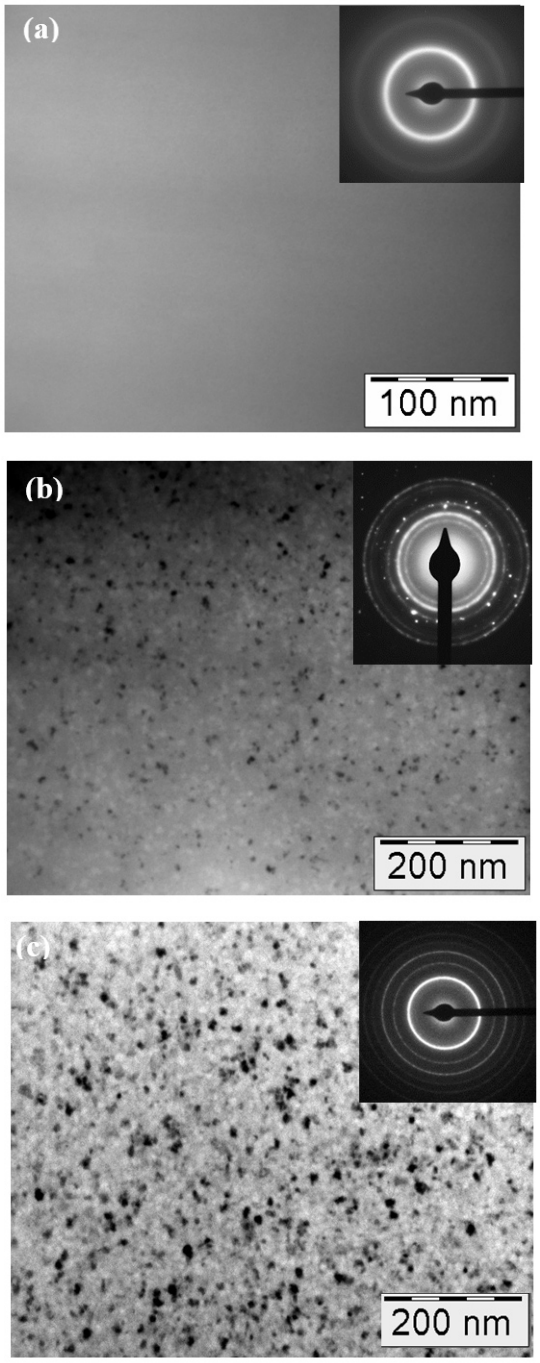

Figure 6. TEM bright field image of (a) $x_{0.1}y_2$ as spun ribbon, (b) $x_{0.1}y_2$ alloy annealed at 610 °C, and (c) $x_{0.35}y_2$ ribbon annealed at 500 °C.

the indexing of the ring pattern observed in the SAD shows the nanograins are of bcc α-Fe(Co) phase. It can be seen that the volume fraction of bcc α-Fe(Co) phase is low validating the volume fraction calculation from XRD results. A rough estimation of volume fraction of nanograins would give 60 to 70 %. Figure 6c shows the TEM BF image of $x_{0.35}y_2$ alloy ribbon annealed at 500 °C. Similar to $x_{0.1}y_2$ alloy ribbon, uniform distribution of bcc α-Fe(Co) phase is seen in the microstructure. Unlike $x_{0.1}y_2$ alloy ribbon, the population of nanograins in the $x_{0.35}y_2$ alloy ribbon annealed at 500 °C is very dense. General trend in the FeCoZrBCu nanocrystalline alloys

is that the dense population of nanograins of bcc α-Fe(Co) phase form on annealing[4-5].

It is interesting to note that only $x_{0.35}$ alloy follows that general trend while $x_{0.1}$ alloy does not. This can be understood considering the elements parting into the amorphous phase or nanocrystalline phase during annealing. In nanocrystalline alloys, Cu becomes fine clusters in the amorphous matrix during solidification which acts as a heterogeneous nucleation sites for the nanocrystalline grains to form and grow. Many studies reported that Fe becomes the core of the nanocrystalline grains and hence it is present in the nanocrytalline phase. As already proved through precision lattice parameter calculations, $x_{0.1}$ alloy having the lattice parameter close to pure Fe value, all other elements are expected to be present in the amorphous phase during the formation bcc α-Fe(Co) phase. Since Zr (1.6 Å) and V (1.44 Å) being heavier atoms than that of many other elements present in the alloy i.e. Fe = 1.26 Å, Co=1.18 Å, and B=0.85 Å, their presence in the amorphous phase decreases the long range diffusion of Fe atoms which would otherwise be required for the formation of bcc α-Fe(Co) phase. Because of aforesaid reasons, the volume fraction of α-Fe(Co) phase formation during the annealing is low in $x_{0.1}$ alloys. As proven through precision lattice parameter calculations, Zr tends to get into the FeCo phase forms on annealing in $x_{0.35}$ alloys. Hence, long range diffusion of Fe would be easy causing the high volume fraction formation of α-Fe(Co) phase.

3.2 Magnetic Properties

Figure 7 (a) & (b) shows the thermomagnetic curves of $x_{0.1}$ and $x_{0.35}$ alloys obtained in VSM at an applied field of 50 Oe. In $x_{0.1}$ alloy series, a sudden decrease of magnetization is observed in all alloys in the range of 120 to 200 °C which corresponds to the ferromagnetic to paramagnetic transition of amorphous phase i.e. Curie temperature (T_c) of the amorphous phase. It can be noted that the T_C of amorphous phase decreases with increase in V content in $x_{0.1}$ alloys. V being non-magnetic atom, while replacing magnetic Fe and Co elements in the composition, it reduces the curie temperature of the amorphous phase.

According to the following equation, the Curie temperature is strongly dependant on the exchange interaction of magnetic atoms (J_{ex})[17].

$$J_{ex} = \frac{3kT_c}{2zS(S+1)} \quad (3)$$

where, z, S and k are number of nearest neighbours, spin (1/2) and constant, respectively. Exchange interaction can be understood using Bethe-Slater curve which gives the exchange interaction of the values Fe, Co, Ni and Mn atoms. When the bigger size V atoms (atomic size: 1.44 Å) replacing the Fe (atomic size: 1.26 Å) and Co (atomic size: 1.18 Å) atoms, the effect of V with other non-magnetic elements of Zr, B and Cu, would be to increase the Fe-Fe distance so much that the exchange interaction reduces. This leads to the decrease in the T_C of amorphous phase with V addition.

Similar to $x_{0.1}$ alloys, ferromagnetic to paramagnetic transition is observed in $x_{0.35}$ ribbons ranges of 420 to 520 °C which correspond to the Curie temperature (T_c) of the amorphous phase. The T_c of amorphous phase decreases with increase in V content similar to $x_{0.1}$ alloy ribbons for the similar reason mentioned early. The T_c of amorphous phase of $x_{0.35}$ alloys is higher than that $x_{0.1}$ alloys due to the high Co content having high T_c (1115°C) than Fe (768°C) in the $x_{0.35}$ alloys.

The saturation magnetization values (at 5 kOe) are plotted as a function of annealing temperature and given in Fig. 8 (a&b) for $x_{0.1}$ and $x_{0.35}$ alloys, respectively. From the Fig. 8a, one can see that the saturation magnetization values of as spun ribbons of $x_{0.1}$ alloy are in the range of 0.6 to 1.0 T which increase on the annealing due to the formation of bcc α-Fe(Co) phase

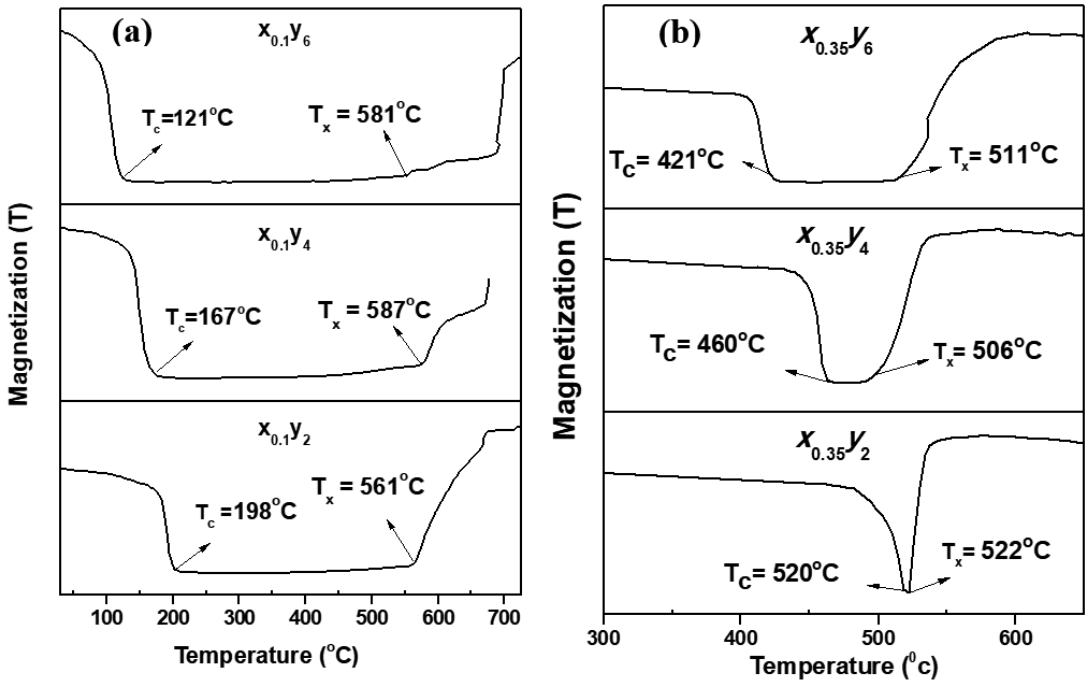

Figure 7. Thermomagnetic curves of as spun ribbons of (a) $x_{0.1}$ and (b) $x_{0.35}$ alloys obtained at an applied field of 50 Oe.

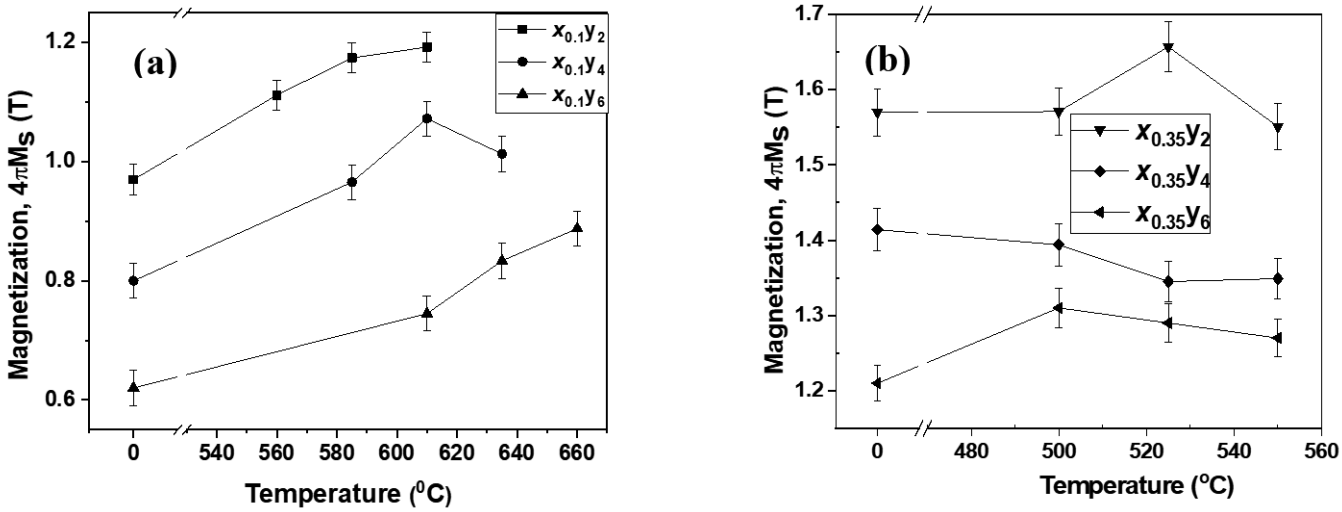

Figure 8. Saturation magnetisation as a function of annealing temperature of (a) $x_{0.1}$ and (b) $x_{0.35}$ alloys.

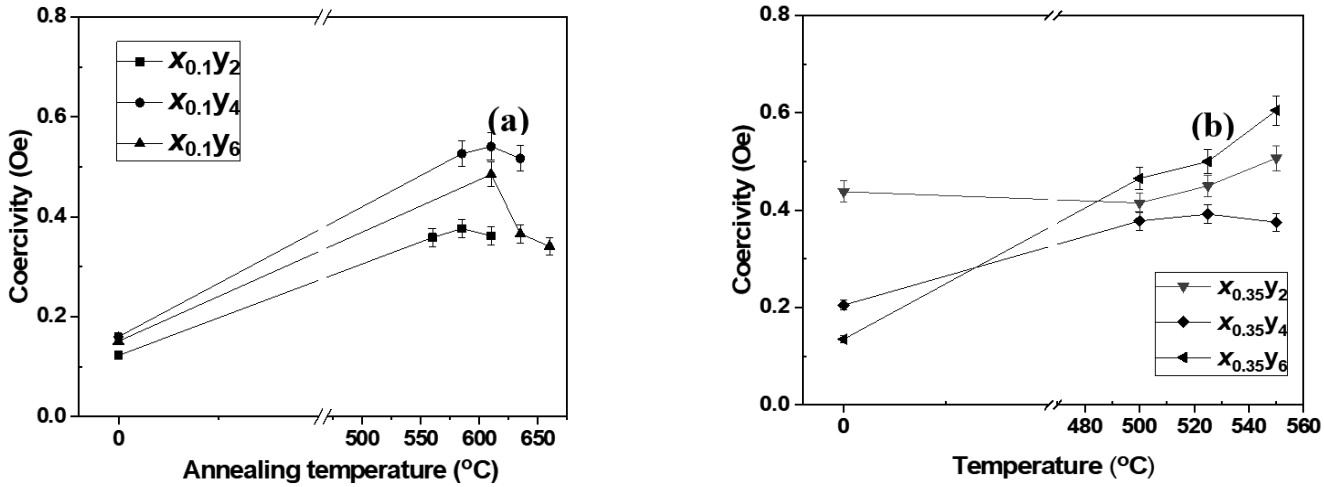

Figure 9. Coercivity as a function of annealing temperature of (a) $x_{0.1}$ and (b) $x_{0.35}$ alloy ribbons.

upto 1.19 T. The amorphous alloys posses low magnetization values due to two reasons namely (i) presence of Fe and Co magnetic elements along with non-magnetic elements in the amorphous phase and (ii) the Tc of amorphous phase is close to room temperature at which the measurement was carried out. The magnetization values decrease with increasing V content and this is due to the non-magnetic nature of V element replacing magnetic Fe and Co elements FeCoZrBCu alloys possess very high magnetization value as high as 1.8 to 1.9T[9] and however, $x_{0.1}$ alloys shows low magnetization values up to a maximum of 1.19 T. This is due to two reasons. First is that low volume fraction formation of bcc α-Fe(Co) phase as proven through XRD and TEM studies. As this phase has high magnetization value, its presence in low volume fraction reduces the magnetization value considerably. Second is that formation of Fe_2Zr phase with low magnetization value whose presence further reduces the magnetization values.

The magnetization values of $x_{0.35}$ alloys are much higher than that of $x_{0.1}$ alloys and the values are in the range of 1.2 T to 1.65 T. The higher magnetization values are due to the reason that FeCo alloys show high magnetization at $Fe_{0.65}Co_{0.35}$ and Fe:Co ratio in $x_{0.35}$ alloys also is same. According to band theory of solids, the maximum magnetic moment which is the difference between the up-spin and down-spin electrons moments, is observed at the composition of $Fe_{0.65}Co_{0.35}$ and hence shows highest magnetization.

In $x_{0.35}$ alloys also, the magnetization values decrease with increasing V content for the same reason mentioned for $x_{0.1}$alloys. Unlike $x_{0.1}$ alloys, the increase in magnetization upon annealing is not much in the case of $x_{0.35}$ alloys. The magnetization values of these alloys are almost similar to the nanocrystalline alloys of $x_{0.35}y_0$[9]. This is due to the fact that T_c of amorphous phase is close to the room temperature (around 60 ^{o}C) in $x_{0.1}$ alloys and the magnetization is very low near T_c and hence shows low magnetization at room temperature. This alloy forms bcc α- Fe phase having high magnetization and high T_c (770 ^{o}C) on annealing and this increases the magnetization drastically when it is measured at room temperature. If the measurement was done at far below room temperature (which is also far below than the T_c of amorphous phase), the increase in magnetization would not be drastic and the extent of increase in magnetization decreases with decrease in temperature. This

behavior is more pronounced in $x_{0.35}$ alloy having high T_c ranging from 421 to 520°C which shows almost slight or no increase in magnetization.

Figure 9(a) shows the variation of coercivity as a function of annealing temperature of $x_{0.1}$ alloys. One can observe that the coercivity value of as spun ribbons are in the range of 0.12 to 0.15 Oe which are equivalent to the coercivity values of FeZrBCu amorphous alloys[3,4] and however the coercivity values of annealed ribbons increase drastically to higher values in the range of 0.35 to 0.55 Oe. In case of nanocrystalline alloys, the annealing leads to the formation of densely populated nano grains in the amorphous matrix and this leads to the exchange interaction between the nano grains through amorphous matrix which reduces the coercivity on annealing due to the averaging out of magnetocrystalline anisotropy by the number of grains. For exchange interaction to take place, the distance between the nanograins to be in the order of ferromagnetic exchange length (L_{ex}) which happens to be few tens of nm for Fe based alloys. However, in the present study, the volume fraction of nanograins is approximately in the range of 60 to 70 % which is not sufficient enough to cause exchange interaction through amorphous phase and this leads to the increase in the coercivity on annealing in these alloys.

Figure 9(b) shows the variation of coercivity as a function of annealing temperature of $x_{0.35}$ alloy ribbons. In these alloys, the coercivity values of as spun amorphous ribbons decrease with increasing V content. Since as spun ribbons with only amorphous phase possess almost zero magnetocrystalline anisotropy (K_1), the possible reason for the reduction of coercivity with increase in V content, may be the reduction in magnetostriction. The coercivity values of annealed ribbons either increase or remain almost constant. It is worth noting that a coercivity of 0.13 Oe is obtained in the $x_{0.35}y_6$ alloy ribbon in the as spun condition which is lower than the coercivity values reported among FeCoZrBCu alloys[3,4]. A combination of good soft magnetic properties obtained in V containing alloys has shown potential for practical applications in magneto-electric technical devices.

4. CONCLUSIONS

The glass forming ability, structure and soft magnetic properties of melt spun ribbons of $(Fe_{1-x}Co_x)_{88-y}V_yZr_7B_4Cu$ with $x_{0.1}y_2$, $x_{0.1}y_4$ and $x_{0.1}y_6$ & $x_{0.35}y_2$, $x_{0.35}y_2$ and $x_{0.35}y_6$ have been investigated. The salient points are summarized and presented here,

- In melt spinning, the structure was found to be fully amorphous for all the ribbons processed at a wheel speed of 47 m/s. Glass forming ability (GFA) of these alloys increase marginally with increase in V content in both x0.1 and x0.35 alloys and Co addition decrease the GFA
- Annealing of amorphous ribbons of $x_{0.1}$ alloys, leads to the formation of bcc α-Fe(Co) phase as a major phase and Fe_2Zr phase as a minor phase in the amorphous matrix, while annealing of amorphous ribbons of $x_{0.35}$ alloys leads to the formation of only bcc α-Fe(Co) phase in the amorphous matrix
- Precision lattice parameter calculations revealed that V addition influences the phase formation in $x_{0.1}$ alloys. It leads to low volume fraction of bcc α-Fe(Co) phase and promotes Fe_2Zr phase
- T_C of amorphous phase increases with Co content and decreases with increasing V addition
- $x_{0.35}$ alloys have higher M_s values than that of $x_{0.1}$ alloy due to higher Co content and however the M_s decreases with increasing V content due to the non-magnetic nature of V
- Coercivity increases with annealing in all V added alloys due to the low volume fraction formation of bcc α-Fe(Co) phase and Fe_2Zr phase. The coercivity decreases with increasing V addition in $x_{0.35}$ alloys as spun ribbons and a lowest coercivity of 0.13 Oe has been obtained in $x_{0.35}y_6$ alloy which is one of the lowest among the similar alloys reported in the literature

REFERENCES

1. Yoshizawa, Y.; Oguma, S.; & Yamauchi, K.; New Fe based soft magnetic alloys composed of ultra fine grain structure. *J. Appl. Phys* 1998, **64**(10), 6044-6046. doi: 10.1063/1.342149
2. Suzuki, K.; Makino, A., Kataoka; N.; Inoue, A.; & Masumoto. T.; High saturation magnetization and soft magnetic properties of bcc Fe-Zr-B and Fe-Zr-B-M (M5transition metal) alloys with nanoscale grain size. *Mater. Trans. JIM*. 1991, **32**, 93. doi: 10.1063/1.350006
3. McHenry, M.E.; Willard, M.A.; & Laughlin, D.E.; Amorphous and nanocrystalline materials for applications as soft magnets. *Prog. Mater. Sci.* 1999, **44**, 291-433. doi: 10.1016/S0079-6425(99)00002-X
4. Willard, M.A.; Huang, M.Q.; Laughlin, D.E.; McHenry, M.E.; Cross, J.O.; Harris, V.G.; & Franchetti, C.; Magnetic properties of HITPERM (Fe,Co)88Zr7B4Cu1 magnets. *J. Appl. Phys.* 1999, **85**, 4421-4423. doi: 10.1063/1.369804
5. Williard, M.A.; Laughlin, D.E.; McHenry, M.E.; Thomas, D.; Sickafus K.; Cross, J.O.; & Harris, V.G.; Structure and magnetic properties of $(Fe_{0.5}Co_{0.5})_{88}Zr_7B_4Cu_1$ nanocrystalline alloys. *J. Appl. Phys*. 1998, **84**, 6773-77. doi: 10.1063/1.369007
6. McHenry, M.E. & Laughlin, D.E.; Nano-scale materials development for future magnetic applications. *Acta Mater.* 2000, **48**, 223-238,. doi: 10.1016/S1359-6454(99)00296-7
7. Williard, M.A.; Laughlin, D.E.; & McHenry, M.E.; Recent advances in the development of $(Fe,Co)_{88}M_7B_4Cu_1$ magnets. *J. Appl. Phys*. 2000, **87**, 7091-7096. doi: 10.1063/1.372941
8. Arvindha Babu, D.; Srivastava A.P.; Majumdar, B., Srivastava D., & Akhtar, D.;: Influence of melt-Spinning parameters on the structure and soft magnetic properties of $(Fe_{0.65}Co_{0.35})_{88}Zr_7B_4Cu_1$ alloy. *Metall. Mater. Trans. A.* 2010, ***41A***, 1313-20. doi: 10.1007/s11661-009-0159-9
9. Arvindha Babu D.; Majumdar, B., Sarkar, R., Manivel Raja, M. and Akhtar, D.; Nanocrystallization of Amorphous $(Fe_{1-x}Co_x)_{88}Zr_7B_4Cu_1$ Alloys and Their Soft Magnetic Properties, *J. Mater. Res*. 2011. **26**(16), 2065-2071, doi: 10.1557/jmr.2011.166
10. R. Parsons, Z. Li, K. Suzuki, Nanocrystalline soft magnet-

ic materials with a saturation magnetization greater than 2 T, J. of Magn. and Magn. Mater. 2004, **278**(1), 299–305. doi: 10.1016/j.jmmm.2019.04.052

11. X.S. Li, Z.Y. Xue, X.B. Hou, G.Q.Wang, X.Huang, H.B.Ke, B.A.Sun, & W.H.Wang, FeCo-based amorphous alloys with high ferromagnetic elements and large annealing processing window, Intermetallics. 2021, **131**(1), 107087-107095. doi: 10.1016/j.intermet.2021.107087
12. Fan, X.; Tang, Y.; Shi, Z.; Jiang, M.; & Shen, B.; The effect of Ni addition on microstructure and soft magnetic properties of FeCoZrBCu nanocrystalline alloys. *AIP Advances* 2017, **7**(5) 056107-1 to 6. doi:10.1063/1.4977229
13. Yu, W.; Zeng, H.; Sun, Y.; Hua, Z.; Effect of Mo addition on the thermal stability, microstructure and magnetic property of FeCoZrBCu alloys. *Vacuum*. 2017, **137**(C), 175-182. doi: 10.1016/j.vacuum.2016.12.048
14. Mitra, A.; Kim, H.-Y.; Louzguine, D.V.; Nishiyama, N.; Shen, B. & Inoue, A.; Structure and magnetic properties of amorphous and nanocrystalline $Fe_{40}Co_{40}Cu_{0.5}Zr_9Al_2Si_4B_{4.5}$ alloys. *J. Mag. & Magnetic Mater.* 2004, **278**(3), 299–305. doi: 10.1016/j.jmmm.2003.12.1315
15. Blazquez, J.S.; Conde, C.F.; Franco, V.; Conde, A. & Kiss L.F.; Magnetic permeability of $(FeCoGe)_{88}Zr_6B_5Cu_1$ alloys: Thermal stability in a wide temperature range. *J. Appl. Phys*. 2008, **103**(7), 07E721-1 to 3. doi: 10.1063/1.2828719
16. Srivastavaa, A.P.; Arvindha Babu, D.; Vermaa, A.; Deshmukhc, A.A.; Kaushala, A. & Palikundwarc, U.A.; Understanding the effect of Hf on thermal stability and glass forming ability of $Fe_{57.2}Co_{30.8}Zr_{7-x}Hf_xB_4Cu_1$ (x = 3, 5, and 7) metallic glasses. *J. Non-Cryst. Solids.* 2018. **503-504**, 7-12. doi: 10.1016/j.jnoncrysol.2018.09.016
17. Cullity, B.D. & Graham, C.D. Introduction to Magnetic Materials, John Wiley & Sons, Inc., Hoboken, New Jersey, USA, 2009.
18. Rao, B.R., Srinivas, M., Shah, A.K., Gandhi, A.S. & Murty, B.S. A new thermodynamic parameter to predict glass forming ability in iron based multi-component systems containing zirconium, *Intermetallics* 2013. **35**, 73-81. doi: 10.1016/j.intermet.2012.11.020
19. Niessen, A.K.; deBoer, F.R.; Boom, R.; deChatel, P.F.; Mattens, W.C.M. & Miedema, A.R.; Model Predictions for the Enthalpy of Formation of Transition Metal Alloys II. *Calphad.* 1983. **7**(1), 51-70. doi: 10.1016/0364-5916(83)90030-5
20. de Boer, F.R.; Boom, R.; Mattens, W.C.M.; Miedema, A.R.; & Niessen, A.K.; *Cohesion in Metals: Transition Metal Alloys*, Ed. de Boer, E.R. & Pettifor, D.G.; North Holland, 1988.
21. Mansoori, G.A.; Carnahan, N.F.; Startling, K.E. & Leland, T.W.Jr.; Equilibrium Thermodynamic Properties of Hard Spheres, *J. Chem. Phys.,* 1971. **54**(4), 1523-1525. doi: 10.1063/1.1675048
22. Arvindha Babu, D.; Majumdar, B.; Sarkar, R.; Murty, B.S. & Chattopadhyay, K.; On the Structural Stability of Melt Spun Ribbons of $Fe_{95-x}Zr_xB_4Cu_1$(x = 7 and 9) Alloys and Correlation with Their Magnetic Properties. *Metall. Mater. Trans. A.,* 2015. **47A**, 560-572. doi: 10.1007/s11661-015-3204-x
23. Nelson, J.B. & Riley, D.P. An experimental investigation of extrapolation methods in the derivation of accurate unit-cell dimensions of crystals. *Proc. Phys. Soc, 1945.* **57**(3), 160-177. doi: 10.1088/0959-5309/57/3/302.

ACKNOWLEDGEMENT

The authors are thankful to Dr G Madhusudhan Reddy, Director, DMRL for encouraging us to publish this work. The authors are also grateful to Dr AK Singh for XRD studies and Dr Rajdeep Sarkar for TEM studies.

CONTRIBUTORS

Mr D. Atchyuth Kumar obtained his M.Tech in Nano Technology from MNIT, Bhopal. His research interests are magnetic materials, nano-crystalline materials, phase field modeling and smart materials.
He has carried out the processing and characterization of samples for this study.

Dr Saijyothi N. obtained her PhD in Metallurgical and Materials Engineering from NIT, Warangal in 2022. Currently she is working in the department of Research and Development (R&D) at Plansee, HPM Pvt. Ltd., Mysore. Her research interests are bulk metallic glasses and structure-property correlations of materials.
She has assisted in determining the glass forming ability of alloys and in drafting the manuscript.

Dr D. Arvindha Babu obtained his PhD in Metallurgical and Materials Engineering from IIT Madras in 2018. He is working as Scientist at DRDO-DMRL.
He has conceptualised this study and designed the experimental methodology and thorough review of the manuscript.

Dr J. Arout Chelvane obtained his PhD in Physics from IIT Madras. He is working as Scientist at DRDO-DMRL, Hyderabad.
He has helped in magnetic experiments.

Dr M. Manivel Raja is working as a Scientist G in at DRDO-DMRL, Hyderabad.
He has helped in technical analysis and manuscript drafting.

Dr T.K. Nandy obtained his PhD in Metallurgical Engineering from IIT BHU. He is working as a Scientist at DRDO-DMRL, Hyderabad. His research interest includes tungsten heavy alloys, titanium alloys and intermetallics.
He has helped in technical analysis and manuscript drafting.